JOURNAL OF Applied Polymer SCIENCE

Removal of Copper(II) from an Aqueous Solution with Copper(II)-Imprinted Chitosan Microspheres

Tao Feng,[1] Jie Wang,[1] Fan Zhang,[1] Xiaowen Shi[2]

[1]College of Resources and Environmental Engineering, Wuhan University of Science and Technology, Wuhan 430081, China
[2]Hubei Biomass-Resource Chemistry and Environmental Biotechnology Key Laboratory, Wuhan University, Wuhan 430079, China
Correspondence to: T. Feng (E-mail: fengtaowhu@163.com)

ABSTRACT: Ion-imprinted chitosan (CS) microspheres (MIPs) were prepared with Cu(II) as a template and epichlorohydrin as a crosslinker for the selective separation of Cu(II) from aqueous solution. The microspheres showed a higher adsorption capacity and selectivity for the Cu(II) ions than nonimprinted chitosan microspheres (NMIPs) without a template. The results show that the adsorption of Cu(II) on the CS microspheres was affected by the initial pH value, initial Cu(II) concentration, and temperature. The kinetic parameters of the adsorption process indicated that the adsorption followed a second-order adsorption process. Equilibrium experiments showed very good fits with the Langmuir isotherm equation for the monolayer adsorption process. The maximum sorption capacity calculated from the Langmuir isotherm was 201.66 mg/g for the Cu–MIPs and 189.51 mg/g for the NMIPs; these values were close to the experimental ones. The selectivity coefficients of Cu(II) and other metal ions on the NMIPs indicated a preference for Cu(II). © 2012 Wiley Periodicals, Inc. J. Appl. Polym. Sci. 128: 3631–3638, 2013

Received 17 April 2012; accepted 26 July 2012; published online 8 October 2012
DOI: 10.1002/app.38406

INTRODUCTION

Chitosan (CS) is the *N*-deacetylation product of chitin and the second most abundant naturally occurring biopolymer next to cellulose. It has biological and chemical properties such as nontoxicity, biocompatibility, and a high chemical reactivity. CS has many $-NH_2$ groups, which can chelate with many metal ions, including Cu(II), Zn(II), and Pb(II). Muzzareui et al.[1] found that noxious heavy metal ions, such as Hg(II), Cu(II), Ni(II), and Cr(III), could be effectively removed through the $-NH_2$ and —OH groups on the CS molecule. Nowadays, CS is widely used in many forms to adsorb heavy metals from wastewater. However, CS and its modification product have many shortcomings. CS has weak mechanical and chemical properties, and it dissolves easily in acids solutions, such as hydrochloric acid and acetic acid.[2,3] Kawamura et al.[4] reported a crosslinked resin that could be used to absorb metal ions. This crosslinked resin had good mechanical properties, but the adsorption capacity (Q) for metal ions was lower when compared with that of free CS because of the crosslinking of chelating functional groups ($-NH_2$). The selectivity of CS for specified metal ions is also low; it might adsorb all heavy metal ions simultaneously; this restricts its applicability in the removal of the named heavy metals from aqueous solutions.

Molecular imprinting technology is an emerging technology that has attracted much attention in the generation of recognition sites by the reversible immobilization of template molecules on crosslinked macromolecular polymer matrices. It consists of the polymerization of a functional monomer mixed with a template in the presence of a crosslinking agent. Then, the removal of the template leaves an imprinted cavity in the polymer, which provides a selective binding site for this template.[5] Ion-imprinted polymers represent a high selectivity and good affinity for target metal ions. So far, the preparation of many metal-ion-imprinted polymers have been studied extensively; these metal ions include Zn(II),[6] Ni(II),[7] Mg(II),[8] and Cd(II).[9] Although the Cu(II)-ion-imprinted CS method has been reported in some articles,[10,11] Cu(II)-ion-imprinted chitosan microspheres (Cu–MIPs) have seldom been synthesized and applied in the selective removal of Cu(II) from aqueous solutions.

The aim of this study was to prepare Cu–MIPs with Cu(II) as a template and epichlorohydrin as a crosslinker for the selective separation of Cu(II) from aqueous solutions.

EXPERIMENTAL

Materials

CS was supplied by Zhejiang Ocean Biochemical Co. (Yuhuan, China). The degree of deacetylation, as determined by potentiometric analysis, was 90%, and the molecular weight calculated from GPC was 2.3×10^5. The copper acetate, formaldehyde, epichlorohydrin, sodium hydroxide, glacial acetic acid, and

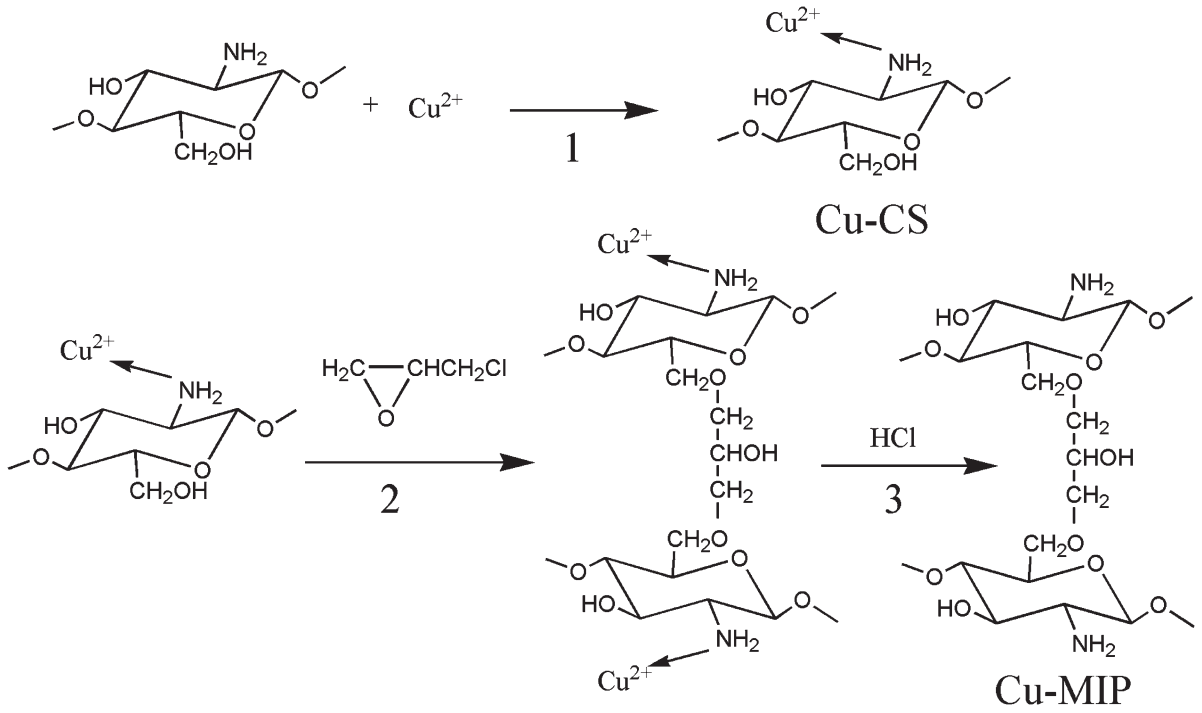

Figure 1. Schemes for the preparation of Cu–CS and Cu–MIPs: (1) chelated with the template (Cu^{2+}), (2) crosslinked with epichlorohydrin, and (3) removal of the template (Cu^{2+}).

other chemicals were analytically pure. All of the solutions were prepared with distilled water. An HY-6 double-multipurpose speed oscillator (Ronghua Equipment Manufacturing Co., Ltd., Jintan, China) was also used.

Preparation of the Cu–MIPs

A 125-mL 4% (w/v) CS solution was prepared with a 2% (v/v) aqueous acetic acid solution, and a certain amount of copper acetate was added to form CS–copper(II) (Cu–CS) complexes. The complexes were then poured into the dispersion medium, which was composed of 50 mL of liquid paraffin and an emulsifier (Span-80). The mixture was stirred for 30 min to form a water-in-oil dispersion, and formaldehyde was added to the medium. After 2 h, the microspheres were collected and washed consecutively with ether, ethanol, and distilled water. Then, the microspheres were suspended in 200 mL of a 0.067*M* NaOH solution, to which the crosslinking reagent epichlorohydrin (1 g) was added.[12] The reaction was carried out at 70°C for 3 h. Later, the microspheres were filtered and soaked overnight with a 1% hydrochloric acid solution to remove Cu(II) and formaldehyde. The Cu–MIPs were washed and then dried in an oven at 60°C for further analysis and use. The nonimprinted chitosan microspheres (NMIPs) were also prepared without the addition of copper acetate. Figure 1 shows the schemes for the preparation of the Cu–CS and Cu–MIPs.

Characterization

The samples were grounded into a powder for the preparation of KBr pellets. The IR spectra of the powdered samples were recorded on a Nicolet-360 Fourier transform infrared (FTIR) spectrometer (Madison, USA) with KBr pellets. The spectrum was corrected for the background noise.

The surface morphology of the magnetic CS microspheres was investigated with scanning electron microscopy (SEM; Hitachi, S-750, Tokyo, Japan). The freeze-dried microspheres were coated with a thin layer of gold and photographed in the electron microscope.

Batch Adsorption Studies

In general, the adsorption experiments were conducted through the addition of 0.1 g of Cu–MIPs or NMIPs into 100 mL of Cu(II) solutions to 250-mL glass vials. The batch adsorption was carried out on a shaker at 120 rpm at different temperatures and different pH values. After adsorption, the solutions were filtered, and the concentrations of Cu(II) were determined by a GGX-9 atomic absorption spectrometer (Haiguang Equipment Manufacturing Co., Bejing, China). Q and the percentage adsorption (A_d) were calculated as follows:

$$Q = \frac{(C_0 - C) \times V}{1000m} \quad (1)$$

$$A_d\ (\%) = \frac{C_0 - C}{C_0} \times 100 \quad (2)$$

where C_0 and C represent the concentrations of metal ions in solution before and after adsorption (mg/L), respectively, V is the volume of the metal-ion solution (mL), and m is the quantity of dry microspheres (g).

RESULTS AND DISCUSSION

Characterization of Cu–MIP

FTIR spectroscopy has been shown to be a powerful tool for the study of the physicochemical properties of polysaccharides. Figure 2(a–c) shows the IR spectra of the CS, Cu–CS complexes,

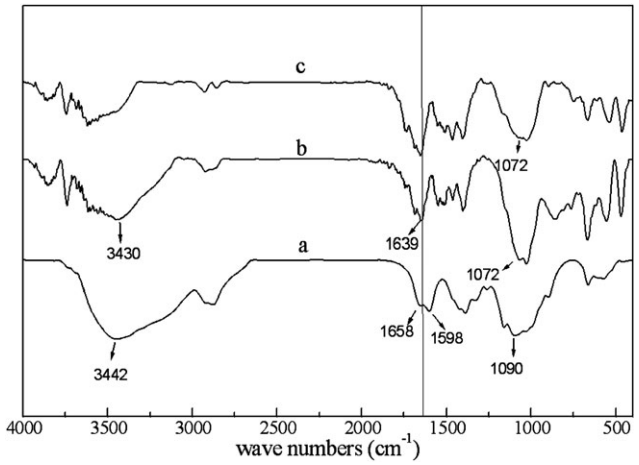

Figure 2. FTIR spectra of the (a) CS, (b) Cu–CS complexes, and (c) Cu–MIPs.

and Cu–MIPs, respectively. Compared to the CS, the wide peak at 3430 cm^{-1}, corresponding to the stretching vibrations of —NH_2 and —OH groups, shifted to a lower frequency in the Cu–CS complexes crosslinked by formaldehyde; this indicated that —NH_2 or —OH groups took part in complexation. The absorption bands at 1660 cm^{-1} assigned to acetamide groups and 1598 cm^{-1} assigned to amine groups disappeared in the complexes. Instead, a new absorption band at 1639 cm^{-1} appeared, which was considered to be characteristic peak of the association of the CS and metal.[13] This suggested that the amine interacted with the metal. The absorption bands at 1072 cm^{-1} assigned to C—O groups weakened and shifted to a lower frequency; this indicated that —OH groups took part in the reaction. The adsorption bands at 3430 and 1072 cm^{-1} in the Cu–MIPs decreased. This showed that the —OH and —NH_2 groups on the CS molecules of the adsorbent surface underwent a derivative reaction with the crosslinking agent.

The morphologies of the Cu–MIPs and NMIPs were observed by SEM. As shown in Figure 3, well-shaped Cu–MIP and NMIP particles were achieved. The NMIPs had a rather smooth surface, whereas the Cu–MIPs displayed a rough surface with many cavities, which indicated that a large number of effective imprinting sites existed on the surface of the Cu–MIPs to rebind the template molecules in aqueous media. *Q* depends mainly on the available immobilized groups, the presence of amorphous domains in the microsphere structure, and the surface area of the adsorbent. The presence of a porous surface structure provided suitable sites for adsorption and led a higher degree of adsorption of the NMIPs.

Effect of the Initial Cu(II) Concentration on the Adsorption

The effect of the initial concentration on the Cu(II) adsorption was tested by the vibration of 100 mL of various Cu(II) concentrations of copper sulfate solution (pH 5.0) and the addition of 0.1 g of adsorbent at room temperature for 12 h.

As shown in Figure 4, the *Q* values of the Cu–MIPs and NMIPs gradually increased as the initial Cu(II) concentration increased until the saturation point was reached at 400 mg/L. The maximum uptake values were 180 and 148 mg/g, respectively; this indicated that the *Q* values of Cu(II) on the CS microspheres was improved significantly by ion imprinting. This high *Q* was attributed to the effective imprinting sites existing on the surface and porous surface structure, which were beneficial for the diffusion of metal ions to the surface and interior regions of the porous microspheres. The porous surface structure also resulted in more surficial effective groups for metal-ion adsorption,

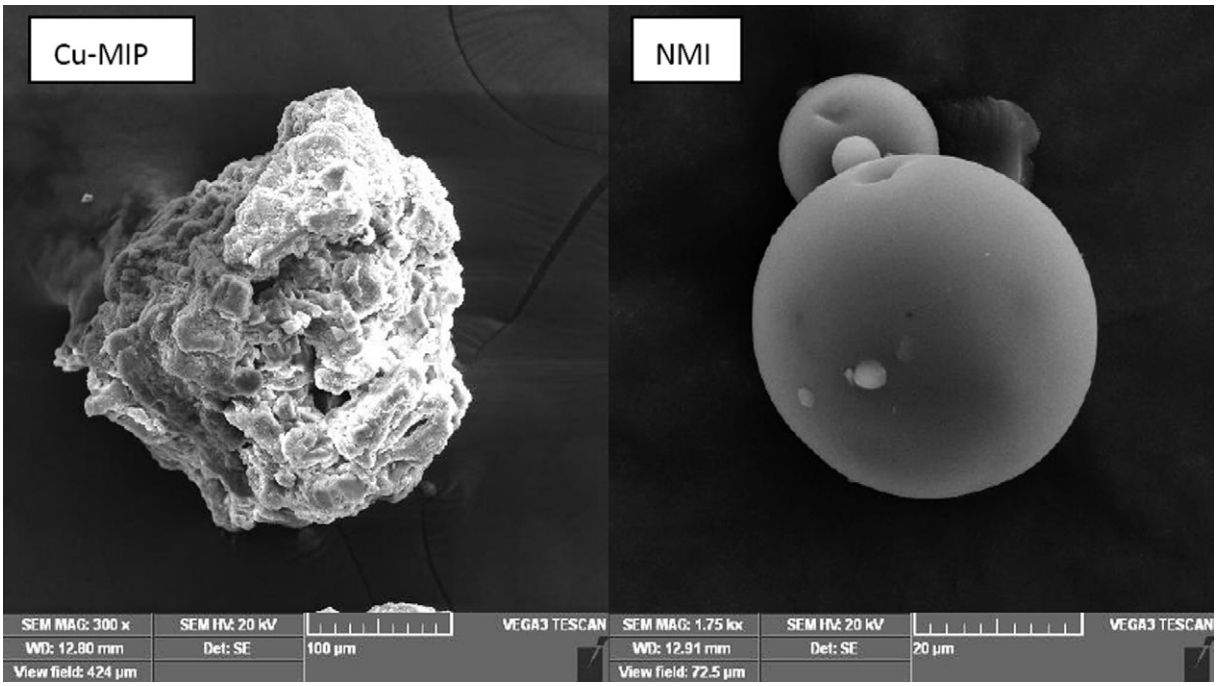

Figure 3. SEM images of the Cu–MIPs and NMIPs.

Applied Polymer SCIENCE

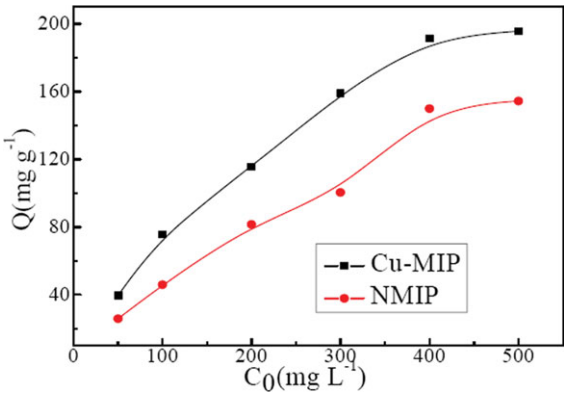

Figure 4. Effect of the initial concentration on the *Q* values of the Cu–MIPs and NMIPs. [Color figure can be viewed in the online issue, which is available at wileyonlinelibrary.com.]

which led to a high *Q*. However, the percentage adsorption [calculated according to eq. (2)] decreased gradually with increasing initial Cu(II) concentration (the data are not shown). These results may be explained by the fact that at high Cu(II) concentrations, more Cu(II) ions were available to adsorb onto the adsorbent before the adsorption–desorption equilibrium was reached. However, at the same time, at high initial Cu(II) concentrations, more Cu(II) ions were left in solution, simply because the total amount of Cu(II) ions was far beyond the *Q* values of the Cu–MIPs and NMIPs.

Effect of the pH on the Adsorption

The effect of the pH on the adsorption of Cu(II) by the Cu–MIPs and NMIPs were investigated at room temperature. The copper sulfate solutions (initial concentration = 400 mg/L) were adjusted to pH 3.0–5.0 and stirred for 12 h.

The results are show in Figure 5. We observed that *Q* increased with increasing contact pH, and the maximum uptake of Cu(II), both in the Cu–MIPs and NMIPs, took place at pH 5. The maximum uptake values were 186 and 151 mg/g, respectively. This was due to competitive adsorption of protons and metal ions onto CS. The uptake of transition metals was mainly affected via coordination with the —NH_2 groups on CS. It was likely that two —OH groups and one —NH_2 group were grabbed by one metal.[14] So, there were

$$M^{2+} + n\mathrm{RNH_2} \Leftrightarrow M(\mathrm{RNH_2})_n^{2+}$$

On the other hand, the —NH_2 of CS reacted with H^+ according to

$$H^+ + \mathrm{RNH_2} \Leftrightarrow \mathrm{RNH_3^+}$$

The low uptake of Cu(II) ions at lower pH was attributed to the high concentration of H^+ ions. Most amine groups of the Cu–MIPs and NMIPs became protonated (—NH^{3+}) at lower pH values; this reduced the number of available binding sites for the sorption of Cu(II). When the pH was increased from pH 3 to pH 5, the amino groups became deprotonated; hence, there were enough binding sites to bind with Cu(II). At pH values higher than 5, the Cu(II) ions of the solution precipitated in the form of $Cu(OH)_2$, which decreased the concentration of Cu(II) ions in solution and influenced the accuracy of the experiment. Thus, a pH of 5 was selected as the optimum pH value of the Cu(II) solution for the following adsorption experiment.

Effect of the Contact Time on the Adsorption

In the test investigating the effect of the contact time on the *Q* values of the Cu(II) experiments, 0.1 g of adsorbent and 100 mL of copper sulfate solution (initial concentration = 400 mg/L and pH 5.0) were used at room temperature. The results are described in Figure 6. A rapid initial rate of sorption on the adsorbents was observed during the first 200 min, and the rate gradually approached limiting sorption after 250 min. The uptakes of the Cu–MIPs and NMIPs were 183 and 157 mg/g, respectively. The main reason for this adsorption rate was that the adsorbents had large surface areas that could supply a large number of binding sites for Cu(II)-ion absorption at the beginning. However, *Q* of Cu(II) became slower in latter stages. This was attributed to the great decrease of the binding sites on the surface of the Cu–MIPs and NMIPs. The surface of the former had many —NH_2 groups that could chelate with Cu(II), but the

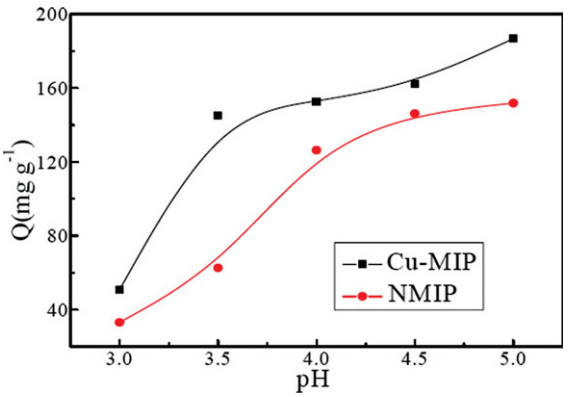

Figure 5. Effect of the pH on the *Q* values of the Cu–MIPs and NMIPs. [Color figure can be viewed in the online issue, which is available at wileyonlinelibrary.com.]

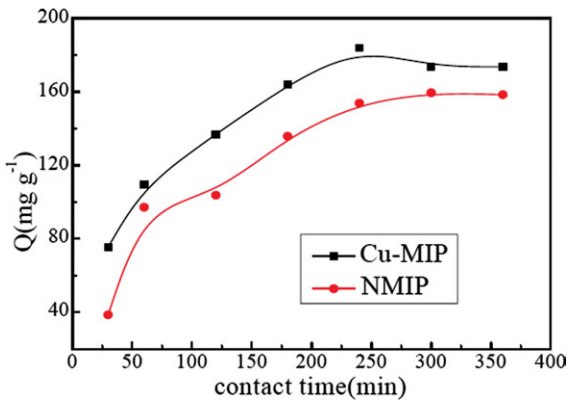

Figure 6. Effect of the contact time on the *Q* values of the Cu–MIPs and NMIPs. [Color figure can be viewed in the online issue, which is available at wileyonlinelibrary.com.]

Table I. Effect of the Temperature on the Q Values and Thermodynamic Parameters of the Adsorption of Cu(II) Ions onto the Cu–MIPs and NMIPs

Adsorbent	Temperature (°C)	Q (mg/g)	ΔG^0 (kJ/mol)	ΔH^0 (kJ/mol)	ΔS^0 (kJ mol^{-1} K^{-1})
Cu-MIPs	10	85.755	−13.197	19.049	0.115
	25	138.585	−15.542		
	35	175.377	−17.055		
	45	181.038	−17.760		
	55	176.321	−18.188		
NMIPs	10	75.377	−12.817	12.089	0.089
	25	129.151	−15.279		
	35	116.887	−15.423		
	45	131.038	−16.361		
	55	134.811	−16.992		

surface of the latter ones only had —OH groups, which did not have enough complexing ability with Cu(II) ions. In addition, as the contract time increased, Cu(II) transferred from the surface of the adsorbents to the inside and accumulated; this slowed down the spreading speed and made the reaction approach equilibrium.

Effect of the Temperature on Q and Adsorption Thermodynamics

The effect of the temperature is an important factor in the sorption process. The effect of the temperature on Cu(II) removal was carried out in 100 mL of copper sulfate solution (initial concentration = 400 mg/L and pH 5.0) through the addition of 0.1 g of adsorbent under various temperatures (10–55°C) for 5 h. Thermodynamic parameters, such as the standard Gibbs free-energy change (ΔG^0), standard enthalpy (ΔH^0), and standard entropy change (ΔS^0), were calculated as follows. The change in free energy of sorption is given by

$$\Delta G^0 = -RT \ln K_c \tag{3}$$

where T is the reaction temperature (K).

The values of ΔH^0 and ΔS^0 were obtained from the slope and intercept of a plot of ln K_c against $1/T$ according to the van't Hoff equation:

$$\ln K_c = \frac{-\Delta H^0}{RT} + \frac{\Delta S^0}{R} \tag{4}$$

where R is the gas constant and K_c is the adsorption equilibrium constant. K_c was calculated from the following equation:[15]

$$K_c = \frac{(Q_0 - Q_c)}{Q_c} \times \frac{V}{m} \tag{5}$$

where Q_0 is the initial concentration of Cu(II) ions in the solution (mg/L), Q_c is the equilibrium concentration of the Cu(II) ions in the solution (mg/L), and V (mL) is the volume of Cu(II)-ion solution.

Table I shows the results. The negative values of ΔG^0 confirmed the spontaneous nature of copper sorption by the sorbents. The positive value of ΔS^0 indicated that the freedom of Cu(II) ions was confused in the sorbents. Table I also shows that the adsorption of Cu(II) ions by the microspheres increased with increasing temperature; this implied that the -adsorption process was endothermic. The positive value of ΔH^0 confirmed it. This may have been due to the fact that when the temperature increased, a greater number of active sites were generated on the microspheres. The process of adsorbing Cu(II) ions broke hydrogen bonds among molecules and within molecules; this was an energy-consuming process. On the other hand, the porosity of the microspheres increased with temperature. The greater the pore sizes were, the smaller the contribution of intraparticle diffusion resistance was. So, an increase in the temperature seemed to decrease the impact of the boundary-layer effect.[16] So, Q was better with higher temperatures.

Selective Adsorption Study

To study the selectivity of Cu(II) ions by the Cu–MIPs and NMIPs, adsorption experiments were carried out with mixed solutions containing Cu(II) and Zn(II), Cu(II), and Pb(II) at equal concentrations (400 mg/L) vibrated at 25°C for 5 h with 0.1 g of adsorbent. The selectivity of the Cu–MIPs and NMIPs for Cu(II) were analyzed from the selectivity coefficient (K), which is defined in the following equation:

$$K = \frac{Q_c}{Q_x} \tag{6}$$

where Q_c is the adsorption capacity of Cu(II) ions by the Cu–MIPs and NMIPs, Q_x is the adsorption capacity of the other metal in the mixed-metal solutions [with Zn(II) or Pb(II)]. The

Table II. Selective Adsorption of the Cu–MIPs and NMIPs

Mixed solution		Cu(II)/Zn(II)		Cu(II)/Pb(II)	
		Cu(II)	Zn(II)	Cu(II)	Pb(II)
NMIPs	Q_1 (mg/g)	93.45	77.24	90.31	66.25
	K_1	1.21		1.36	
Cu-MIPs	Q_2 (mg/g)	172.35	43.68	153.17	31.75
	K_2	3.95		4.82	

Table III. Effect of the Generation Time on the Q Values of Cu–MIP

Generation time	1	2	3	4
Q (mg/g)	182.92	170.66	164.06	156.51

greater the value of K was, the better the selectivity toward Cu(II) over Zn(II) or Pb(II) was. The results are shown in Table II. We observed that the NMIPs had little selectivity for Cu(II) over Zn(II) or Pb(II) in the mixed solution. On the contrary, the Cu–MIPs showed an obviously improved selectivity for Cu(II). This indicated that the Cu–MIPs had the capability of recognizing Cu(II) with a high affinity and selectivity. This was attributed to the Cu(II)-ion-imprinted cavity in the Cu–MIPs, which provided a selective binding site for Cu(II) ions.

Regenerative Adsorption of Cu–MIP

Because traditional adsorbents are difficult to recycle, it is necessary that such adsorbents can be used repeatedly. For the regenerative adsorption studies, 0.4 g of Cu–MIPs and 400 mL of a copper sulfate solution (initial concentration = 400 mg/L) were used. After adsorption, the Cu–MIP-loaded Cu(II) ions were then agitated with a hydrochloric acid solution and washed with deionized water to neutralize the solution. The adsorbents were regenerated four times, and we calculated the regeneration Q with eq. (1). The results are shown in Table III. With increasing regeneration number, Q decreased but still retained more than 90% of its initial value. However, most of the amino groups of the Cu–MIPs became protonated when agitated with hydrochloric acid. So, part of the sites occupied by the metal ions may have been replaced by H^+, and the absorption capacity of the Cu–MIPs could be regenerated. Therefore, the recycled Cu–MIPs had a high capacity for Cu(II) removal during each cycle. Nevertheless, Q decreased in each cycle. This was because some of the Cu–MIPs dissolved during regeneration process, and the number of —OH groups and —NH_2 groups in the Cu–MIPs decreased. This led to the situation that the Cu–MIPs had a poor complexing ability with Cu(II) ions.

Equilibrium Isotherm Models

Equilibrium isotherm equations could be used to describe the experimental sorption data and provide some insight into the sorption mechanism, the surface properties, and the affinity between the sorbent and sorbate.[17] The Langmuir isotherm model assumes monolayer coverage of the adsorbate on a homogeneous adsorbent surface. This model does not consider the surface heterogeneity of the sorbent. It assumes that adsorption will take place only at special site on the adsorbent. The Freundlich isotherm model is an empirical equation that describes the surface heterogeneity of the sorbent. It considers multilayer adsorption with a heterogeneous energetic distribution of active sites, accompanied by interactions between the adsorbed molecules.[18]

The Langmuir isotherm equation follows:

$$\frac{1}{Q_e} = \frac{1}{Q_{\max}} + \frac{1}{BQ_{\max}C_e} \tag{7}$$

where C_e is the equilibrium concentration of metal ions (mg/L), Q_e is the sorption capacity of metal ions (mg/g), $Q_{\max}$ (mg g^{-1}) is the maximum adsorption capacity of the adsorbent, and B (dm^3/mg) is the Langmuir adsorption constant.

The Freundlich isotherm equation is as follows:

$$\ln Q_e = \ln K + \left(\frac{1}{n}\right) \ln C_e \tag{8}$$

where C_e is the liquid-phase Cu(II) concentration at equilibrium (mg/L), k and n are the Freundlich isotherm constant, and $1/n$ (dimensionless) is the heterogeneity factor.

Table IV shows the calculated values of the Freundlich and Langmuir model parameters. The Cu(II) adsorptions with the Cu–MIPs and NMIPs showed good fit with the Langmuir isotherm because of their high R^2 values (R^2 = 0.9947 and 0.9978, respectively). This suggests monolayer coverage of Cu(II) on the surface of the adsorbent. The maximum sorption capacity calculated from the Langmuir isotherm was 201.66 mg/g for Cu–MIP and 189.51 mg/g for NMIP; these values were close to the experimental values. Similar behavior was also found for the adsorption of Cu(II) on the surface-carboxymethylated CS hydrogel beads.[19]

The $Q_{\max}$ values of Cu(II) onto other modified CS adsorbents prepared under different conditions and reported in the literature[20–24] are listed in Table V. We observed that the $Q_{\max}$ value varied considerably for different adsorbents. In this study, the Cu–MIPs showed higher adsorption capacities compared to those of glutaraldehyde (GLA)-crosslinked CS derivatives with Cu(II) or Pb(II) templates. However, GLA-crosslinked CS exhibited better Q values. The varieties of $Q_{\max}$ were mainly derived from the differences in the concentration and volume of the Cu(II) ion solutions. Q increased when the initial dosage of Cu(II) increased. Furthermore, the adsorption of Cu(II) on the MIPs was also dependent on the kinds of crosslinkers and metal-ion templates.

Kinetic Modeling

To investigate the adsorption kinetics, two different kinetics models, pseudo-first-order and pseudo-second-order rate

Table IV. Freundlich and Langmuir Isotherm Constants

	Freundlich adsorption model			Langmuir adsorption model		
Adsorption material	n	K	R^2	$Q_{\max}$	B	R^2
Cu-MIPs	2.1177	14.5889	0.9685	201.66	0.0243	0.9947
NMIPs	1.4520	2.9216	0.9818	189.51	0.0063	0.9978

Table V. Q_{max} Values of Various CS Samples Modified for the Adsorption of Cu(II) as Reported in the Literature

Adsorbent	Concentration of metal ion	Volume	Q_{max} (mg/g)	Reference
ECH-crosslinked Cu–MIPs	400 mg/L	100 mL	201.66	This study
GLA-crosslinked carboxymethyl CS with Cu(II) template	0.02 mol/L	25 mL	156.8	20
GLA-crosslinked *N*-succinyl CS with Pb(II) template	0.02 mol/L	25 mL	175.36	21
GLA-crosslinked Cu–MIPs	0.08 mol/L	50 mL	165.12	22
ECH-crosslinked metal-imprinted CS	10 mg/L	100 mL	19.80	23
GLA-crosslinked CS	0.16–5.04 mmol/L	250 mL	320	24

ECH, epichlorohydrin; GLA, glutaraldehyde.

Table VI. Dynamic Constants of the Two Models

Adsorption material	$q_{e(exp)}$ (mg/g)	Pseudo-first-order kinetics			Pseudo-second-order kinetics		
		k_1	$q_{e(cal)}$ (mg/g)	R^2	k_2	$q_{e(cal)}$ (mg/g)	R^2
Cu–MIPs	183.87	10.9×10^{-3}	152.02	0.9737	1.01×10^{-4}	203.25	0.9952
NMIPs	153.68	11.0×10^{-3}	143.18	0.8590	6.82×10^{-5}	192.31	0.9899

$q_{e(exp)}$, equilibrium adsorption capacity from experiments; $q_{e(cal)}$, calculated equilibrium adsorption capacity from kinetics models.

models, were used in this study. The pseudo-first-order and pseudo-second-order models are given in eqs. (9) and (10), respectively:

$$\log(q_e - q_t) = \log q_e - \frac{k_1}{2.303} \times t \tag{9}$$

$$\frac{t}{q_t} = \frac{1}{k_2 q_e^2} + \frac{t}{q_e} \tag{10}$$

where q_e and q_t (mg/g) are the amounts of Cu(II) ions adsorbed onto the adsorbents at equilibrium and at time t, respectively, and k_1 (min^{-1}) and k_2 (g mg^{-1} min^{-1}) are the rate constants of pseudo-first-order and pseudo-second-order adsorption, respectively.

The calculated parameters of the pseudo-first-order and pseudo-second-order kinetic parameters are given in Table VI. On comparing the R^2 values obtained, we concluded easily that the ongoing reaction proceeded via a pseudo-second-order mechanism rather than a pseudo-first-order mechanism. This indicated that chemisorption might have been the rate-limiting step that controlled these adsorption processes. The pseudo-second-order kinetic equation was also more likely to show that the sorption behavior may have involved valency forces through electron-sharing between the metal ions and adsorbents.[25]

CONCLUSIONS

Cu–MIPs and MIPs were prepared, and the Cu–MIPs showed improved selective adsorption of Cu(II) ions over Zn(II) and Pb(II) ions from aqueous solutions. The batch experiment showed that the adsorption was dependent on pH, contact time, initial Cu(II) concentration, and temperature. The maximum Cu(II) uptake by the Cu–MIPs was achieve at pH 5.0 and was about 180 mg/g; this was much higher than that of the NMIPs (140 mg/g). The adsorption process fit the Langmuir model better than the Freundlich model. The adsorption kinetics were well described by the pseudo-second-order equation. This indicated that the Cu(II) adsorption mechanism of the Cu–MIPs was monolayer chemisorption.

ACKNOWLEDGMENT

Financial support was provided by the National Natural Science Foundational of China (contract grant number 50904047), Wuhan Science and Technology Bureau (contract grant number 201271031420), and Hubei Biomass-Resource Chemistry and Environmental Biotechnology Key Laboratory, Wuhan University (contract grant number HBRCEBL2011-2012002).

REFERENCES

1. Muzzareui, R. A. A.; Weckx, X.; Filippinj, O.; Sigon, F. *Carbohydr. Polym.* **1989**, *11*, 293.
2. Popuri, S. R.; Vijaya, Y.; Boddu, V. M.; Abburi, K. *Bioresour. Technol.* **2009**, *100*, 194.
3. Chen, A. H.; Liu, S. C.; Chen, C. Y. *J. Hazard. Mater.* **2008**, *154*, 184.
4. Kawamura, Y.; Mitsuhashi, M.; Tanibe, H. *Ind. Eng. Chem. Res.* **1993**, *32*, 386.
5. Panahi, R.; Vasheghani-Farahani, R.; Shojaosadati, S. A. *Biotechnol. Adv.* **2008**, *26*, 533.
6. Yoshida, M.; Uezu, K.; Goto, M.; Furusaki, S. *Macromolecules* **1999**, *32*, 1237.
7. Ersöz, A.; Say, R.; Denizli, A. *Anal. Chim. Acta* **2004**, *502*, 91.
8. Dhal, P. K.; Arnold, F. H. *J. Am. Chem. Soc.* **1991**, *113*, 7417.

9. Liu, B. J.; Wang, D. F.; Xu, Y.; Huang, G. Q. *J. Mater. Sci.* **2011**, *46*, 1535.
10. Sun, S. L.; Wang, A. Q. *Sep. Purif. Technol.* **2006**, *49*, 197.
11. Dalida, M. L. P.; Mariano, A. F. V.; Futalan, C. M.; Kan, C. C.; Tsai, W. C.; Wan, M. W. *Desalination* **2011**, *275*, 154.
12. Qin, C.; Du, Y.; Zhang, Z.; Liu, Y.; Xiao, L.; Shi, X. *J. Appl. Polym. Sci.* **2003**, *90*, 505.
13. Wang, X.; Du, Y.; Fan, L.; Liu, H.; Hu, Y. *Polym. Bull.* **2005**, *55*, 105.
14. Juang, R. S.; Shao, H. *J. Adsorption* **2002**, *8*, 71.
15. Chiou, M. S.; Li, H. Y. *Chemosphere* **2003**, *50*, 1095.
16. Chatterjee, S.; Lee, D. S.; Lee, M. W. *Bioresour. Technol.* **2009**, *100*, 2803.
17. Krishna, B. S.; Murty, D. S. R.; Prakash, B. S. J. *J. Colloid Interface Sci.* **2000**, *229*, 230.
18. Vimonsesa, V.; Lei, S.; Jin, B. *Chem. Eng. J.* **2009**, *148*, 354.
19. Yan, H.; Dai, J.; Yang, Z.; Yang, H.; Cheng, R. *Chem. Eng. J.* **2011**, *174*, 586.
20. Sun, S.; Wang, A. *Sep. Purif. Technol.* **2006**, *49*, 197.
21. Sun, S.; Wang, Q.; Wang, A. *Biochem. Eng. J.* **2007**, *36*, 131.
22. Cao, Z.; Ge, H.; Lai, S. *Eur. Polym. J.* **2001**, *37*, 2141.
23. Chen, C. T.; Yang, C. Y.; Chen, A. H. *J Environ. Manage.* **2011**, *92*, 796.
24. Osifo, P. O.; Webster, A.; Merwe, H. V. D.; Neomagus, H. W. J. P.; Gun, M. A. V. D.; Grant, D. M. *Bioresour. Technol.* **2008**, *99*, 7377.
25. Niu, C.; Wu, W.; Wang, Z.; Li, S.; Wang, J. *J. Hazard. Mater.* **2007**, *141*, 209.